Nuclear Inst. and Methods in Physics Research, A 966 (2020) 163838

Contents lists available at ScienceDirect

Nuclear Inst. and Methods in Physics Research, A

journal homepage: www.elsevier.com/locate/nima

Test and simulation of a Cherenkov picosecond timing counter

Ziwei Li, Xin Li *, Qiang Cao, Cheng Li, Yonggang Wang, Jianbei Liu, Ming Shao, Haiping Peng, Xu Wang, Yi Zhou, Zhengguo Zhao

State Key Laboratory of Particle Detection and Electronics, University of Science and Technology of China, Hefei 230026, China
Department of Modern Physics, University of Science and Technology of China, Hefei 230026, China

ARTICLE INFO

Keywords:
Picosecond timing
Multi-threshold differential discriminator
Cherenkov radiation
GEANT4 simulation

ABSTRACT

To study the picosecond timing technology, a counter with compact structure, fast timing, and relatively low material budget has been developed. The prototype is composed of Cherenkov radiator, micro-channel plate photoelectron multiplier tube (MCP-PMT), and fast readout electronics. The readout electronics consists of a programmable differential amplifier, a multi-threshold differential discriminator, and a timestamp Time-to-Digital converter implemented in a field-programmable gate array (FPGA). The beam test demonstrates that it can achieve an excellent time resolution around 10ps. Its timing performance is also evaluated by a Geant4 simulation framework. The test and simulation result are consistent and there is still potential for improvement.

1. Introduction

In order to match the increasing energy and luminosity of the new generation particle accelerator, with high-rate and high-momentum particle flux of various final states and large phase space, detectors with unprecedented time and position resolution are required. The Picosecond Timing (PsT) technology, including the fast photoelectric sensors and fast readout electronics for precise 10-ps level timing, has been considered as one of the key breakthroughs in the development of new-generation detectors [1–3]. And it has already been adopted in the development and upgrade of detectors for several experiments. For instance, in the CMS electromagnetic calorimeter upgrade for the HL-LHC experiment, the PsT technology is applied to improve its time resolution to 20∼30 ps by using multiple timing detection layers [4]. It is also considered for the LHCb upgrade, which features a TORCH (Time Of internally Reflected Cherenkov light) detector, aiming at a time resolution of 10∼15 ps per track [5].

To study the PsT technology, we develop a fast timing counter consisting of Cherenkov radiator, fast MCP-PMT, and a full readout electronics chain. The timing performance of the prototype has been tested in the 150 GeV muon beam at CERN/SPS-H4. A Geant4 simulation framework is also developed as a reference to study its working mechanism. The test and simulation results will be discussed in this paper.

2. Timing counter and electronics

The prototype is composed of an MCP-PMT (Hamamatsu, R3809U-50 [6]) coupled to a 15 mm × 15 mm × 38 mm fused silica radiator. We also used a 5 mm × 5 mm × 5 mm radiator of same material coupled to MCP-PMT as the time reference (T0) in the beam test. To simplify the description, we call them TC1 (15 mm × 15 mm × 38 mm radiator + R3809U) and TC0 (5 mm × 5 mm × 5 mm radiator + R3809U) respectively as shown in Fig. 1.

2.1. Fused silica

The fused silica is produced by the Beijing Quartz and Special Glass Institute, which has a transmission rate of 91.3% for ultraviolet light at the wavelength above 300 nm. With an average refractive index of 1.46, the maximum radiation angle of Cherenkov light is 46.8 degrees with a light yield of ∼260/cm in the wavelength range of 300∼400 nm. To be better coupled to R3809U with a round window of 10 mm diameter, one end of the fused silica radiator of TC1 is processed into a cone shape, and the coupling surface is coated with silicone oil (Rhodorsil Huile 47 V 1000) permeable to ultraviolet light. The radiator is wrapped by aluminum foil on four side faces, and by the black paper on the rear end to reduce the time spread from multiple internal reflections of photons.

2.2. MCP-PMT

The performance of R3809U is tested by using a picosecond laser (Passat COMPILER, FWHM = 4 ps, λ = 215 nm). The laser is split into two beams, illuminating the MCP-PMT under test (single-photon mode) and reference MCP-PMT (multi-photon mode, used as the time reference for transit time measurement) respectively, as shown in Fig. 2.

* Corresponding author at: Department of Modern Physics, University of Science and Technology of China, Hefei 230026, China.
E-mail address: li124ste@ustc.edu.cn (X. Li).

https://doi.org/10.1016/j.nima.2020.163838
Received 5 May 2019; Received in revised form 19 March 2020; Accepted 20 March 2020
Available online 26 March 2020

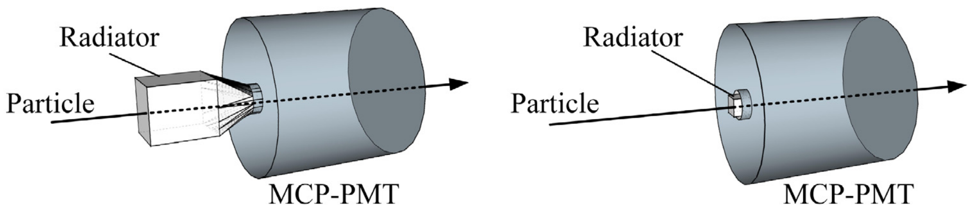

Fig. 1. Timing counter prototype: TC1 (left) and the time reference: TC0 (right).

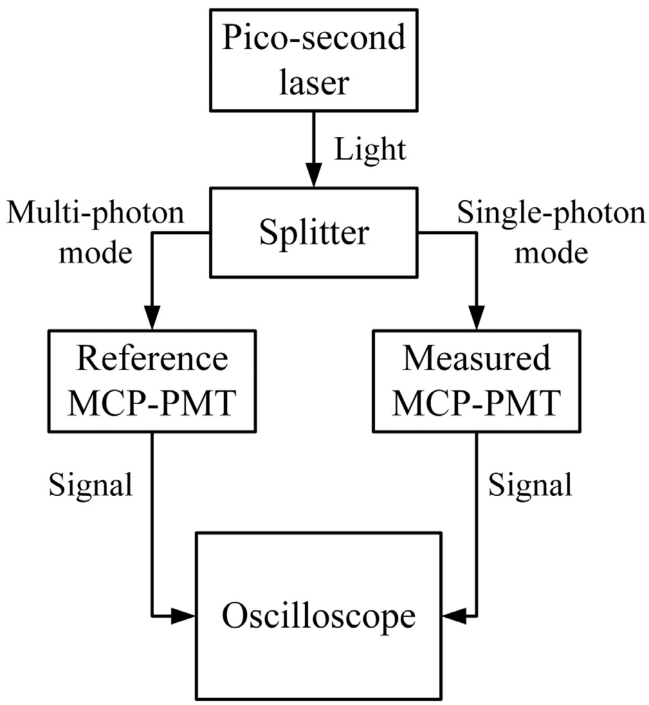

Fig. 2. The test setup to characterize the single-photoelectron properties of MCP-PMT.

A high bandwidth oscilloscope (LeCroy WM813ZI-A, sampling rate: 40 Gs/s) is used to record the output signal waveforms. Fig. 3. shows the performance of MCP-PMT at the high voltage (HV) of 3100 V: Its gain is 1×10^6, calculated by: $Gain = \frac{Q_{PE1}-Q_{ped}}{e}$. Because single photon can possibly induce single, double or triple photoelectrons in PMT, we use a three-Gaussian fit to estimate the contribution of 1st, 2nd, 3rd photoelectron and an exponential fit for pedestal contribution, as shown in Fig. 3. Here Q_{PE1} is the peak charge of 1st photoelectron. Q_{ped} is the peak charge of pedestal led by noise, and e is the single electron charge of 1.6×10^{-19} C. The Transit time spread (TTS) of MCP-PMT is 18 ps, obtained from the time difference between the measured MCP-PMT and reference MCP-PMT.

2.3. Readout electronics

As a crucial part of the picosecond timing technology, the time uncertainty contributed from the front-end electronics is expected as low as several picoseconds. To meet this requirement, an FPGA-based readout electronics with a multi-threshold leading-edge timing scheme is designed. It consists of a gain programmable differential amplifier (PDA), a multi-threshold differential discriminator (MDD), and a set of time-to-digital converters (TDC) as shown in Fig. 4. Except for the PDA and bias network, other components are implemented inside of a field-programmable gate array (FPGA) chip (Kintex-7 from Xilinx).

The output signals of MCP-PMT are amplified by the differential amplifier LMH6881 from Texas Instruments, whose bandwidth is 2.4 GHz with a gain ranging from 6 dB to 26 dB [7]. This amplifier also provides conversion from unipolar input to differential output and transferred the MCP-PMT signal to the MDD module with a strong anti-noise ability.

The MDD module is composed of a resistor-capacitor bias network and a set of high-performance comparators based on Low Voltage Differential Signaling (LVDS) receivers of FPGA. The bias network not only translates the differential signal to the form suitable for LVDS receivers but also provides pre-set thresholds. In the MDD module, the input signals are split into four differential comparators with different thresholds as shown in Fig. 5. All comparators are front-edge timing, their outputs with three lower thresholds are used as event timing samples, evaluating signals' rise time at different thresholds and providing the time-walk correction. Meanwhile, the comparator with the highest threshold provides information for noise rejection. Then the outputs are fed into four channels of TDC respectively.

The TDC module is implemented in the FPGA using a ones-counter encoding scheme, its intrinsic RMS time resolution is evaluated as 3.9 ps [8]. The measured timestamp of the event is packaged and transmitted to the PC for further processing. The intrinsic time performance of the entire electronics is evaluated as 5.6 ps by feeding the same signals into two channels [9].

3. Beam test

3.1. Time resolution

The performance of the prototype has been tested in the 150 GeV muon beam at CERN/SPS-H4. The test setup is shown in Fig. 6. The timing difference between TC1 and TC0 is measured by readout electronics. The measured arrival time is obviously affected by the fluctuation of signal amplitude, so a time–amplitude (T–A) slewing correction is necessary. Since the readout electronics only collect timing information from TDC, we use the rise time between two thresholds instead of the amplitude to make the correction as shown in Fig. 7. The test result after T–A correction with various thresholds is shown in Fig. 8. The time resolution achieves 11.3 ps. By subtracting the electronic uncertainty, its intrinsic timing resolution is:

$$\sigma = \sqrt{{\sigma_{T1-T0}}^2 - {\sigma_e}^2} = \sqrt{11.3^2 - 5.6^2} = 9.8 \text{ ps}.$$

For comparison, the prototype's signals are also read out by the oscilloscope (Leroy WM813ZI-A, sampling rate: 40 Gs/s) using Constant Fraction Discriminator (CFD) technique with constant amplitude fraction as timing threshold, as shown in Fig. 9. The best time resolution of 9.3 ps is obtained at 30% amplitude. Clearly, the readout electronics has excellent time performance.

3.2. Discussion

Without the track information in the beam test, the time resolution of the prototype shown above still includes the uncertainty of track's hit position and can be further improved. Even if without an external radiator, An MCP-PMT itself shows hit-position dependence of the time resolution [10]. As shown in Fig. 10, when the incident particles pass

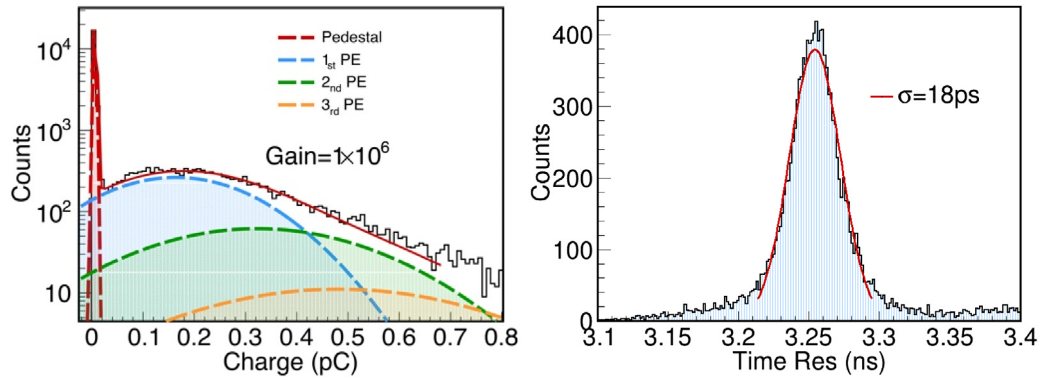

Fig. 3. Measured characteristics of MCP-PMT: Single photoelectron spectrum at HV of 3100 V and Gain of 1×10^6 is calculated (left). Transit time spread (TTS) of 18 ps is obtained from the time difference between measured MCP-PMT and reference MCP-PMT (right).

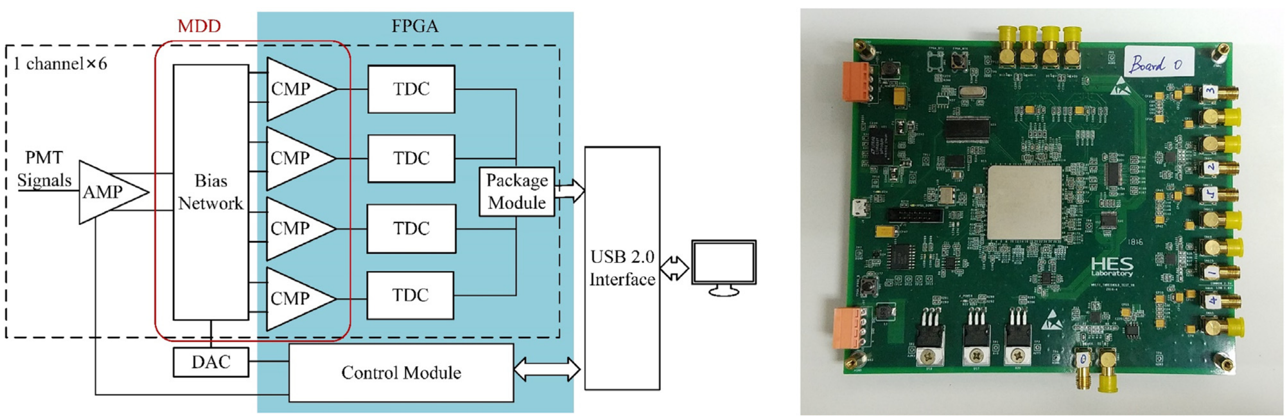

Fig. 4. Schematic diagram (left) and photo of designed electronics (right).

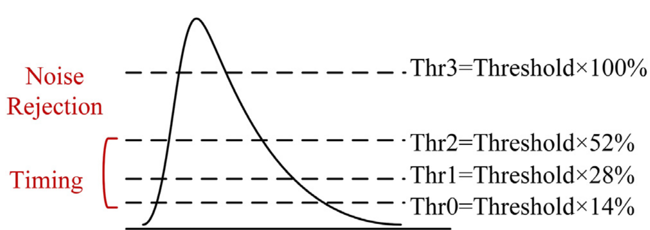

Fig. 5. Schematic diagram of four-threshold setup for signal timing and noise rejection.

through the PMT's window of 3.2 mm thickness,[1] the Cherenkov light cone generated within the innermost circle is fully projected on the photocathode ("Full Signal"), which means all Cherenkov photons can directly reach the photocathode without any reflection and induce fast signal. On the other hand, the cone generated by the outer circle is partially projected on ("Partial Signal") or only reaches the photocathode by reflection ("Reflected Signal"), which means part or full of the cone reaches the photocathode by multiple reflections and induces relatively slow signals. So the "Full Signal" is from direct-hit photons, the "Partial Signal" is from both direct-hit photons and reflected photons, and the

[1] From R3809U datasheet (HAMAMATSU).

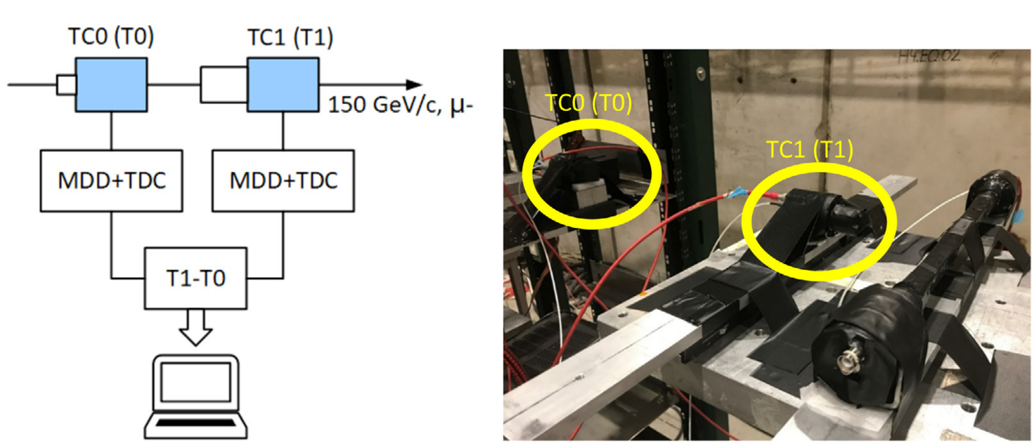

Fig. 6. Setup of beam test in H4 beam line (left) and photo of timing counters at CERN/SPS-H4 (right).

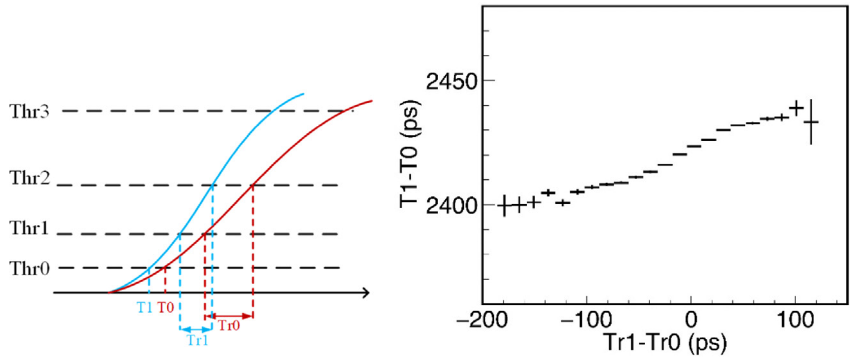

Fig. 7. (left) The arrival time difference between TC0 & TC1 (T1–T0) and their rise time difference (Tr1–Tr0) at threshold of; (right) The rise time correlation (Tr1–Tr0) vs. (T1–T0)..

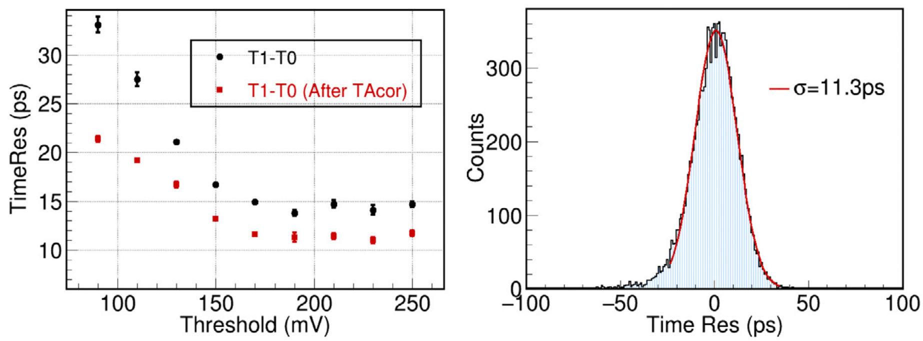

Fig. 8. The Gaussian-fit time resolution (T1–T0) with or without T–A correlation as a function of timing threshold (left) and the best resolution is at the threshold of 230 mV: $\sigma = 11.3$ ps (right).

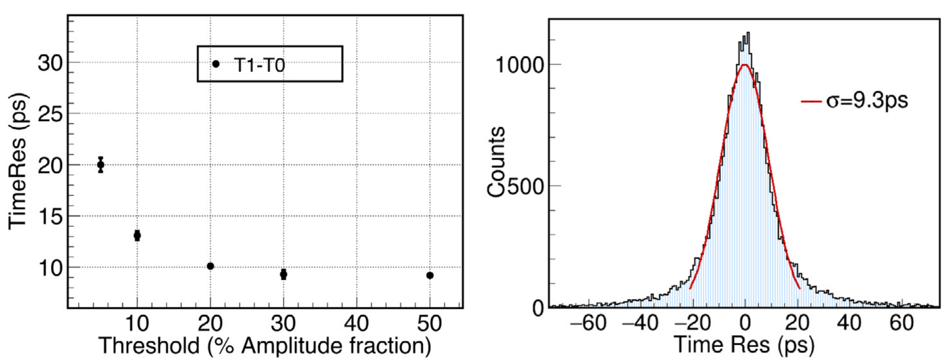

Fig. 9. The Gaussian-fit time resolution (T1–T0) as a function of timing threshold (% amplitude fraction) (left) and the best resolution at a threshold of 30% amplitude: $\sigma = 9.3$ ps (right).

"Reflected Signal" is from reflected photons. Considering the size of the photocathode and the thickness of PMT's window, the Cherenkov light cone is fully projected on the photocathode in the diameter <5 mm, partially projected in the diameter range of 5 mm∼17 mm, and reaches the photocathode only by reflection in the diameter >17 mm.

The arrival time difference among these three kinds of signals will cause timing fluctuation. To analyze their influence on the prototype's timing performance, a GEANT4 simulation has been developed to characterize the position dependence of the prototype's time resolution.

4. Monte Carlo simulation

4.1. Simulation process

Base on the GEANT4 framework, a timing counter simulation is developed including the majority of physics process: Cherenkov radiation and optical transmission [11]. The output signal waveform is simulated based on the GEANT4 hit information and the response function of MCP-PMT [12]:

$$V_{PMT}(t) = \sum_{i=1}^{N_{pe}} v_i(t - t_{TTS} - t_{arr,i}),$$

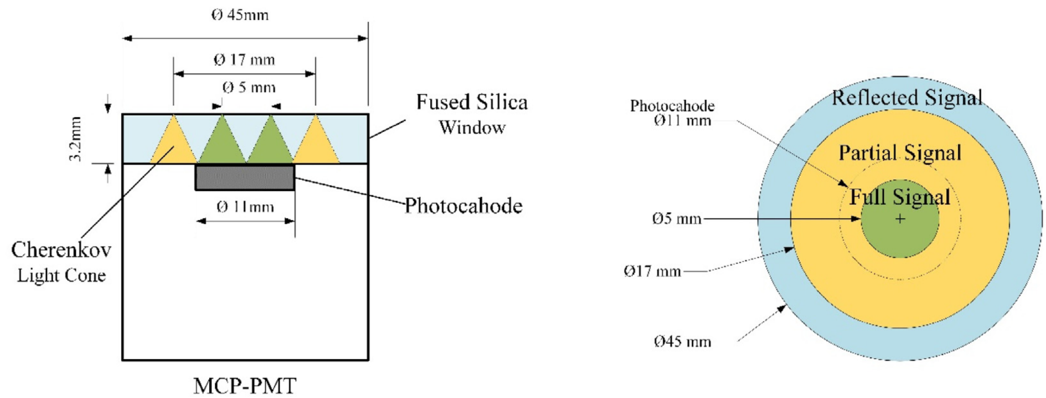

Fig. 10. R3809U dimensional outline (left) and its photocathode projected by Cherenkov cone (right).

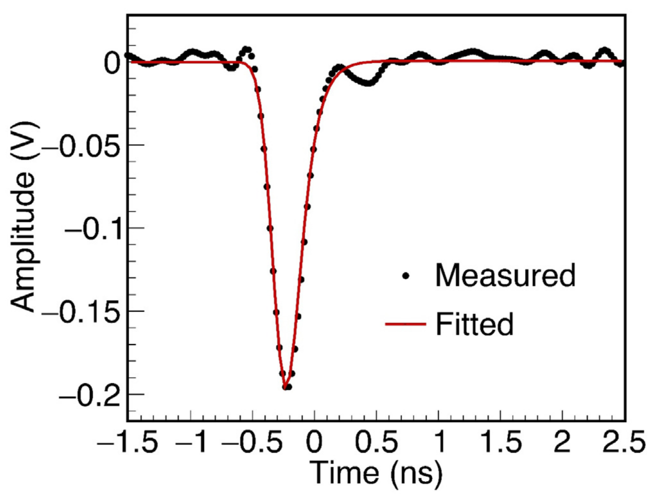

Fig. 11. The simulated SPE response of MCP-PMT (red line) [13] and an example response measured by the oscilloscope (black line).

where t_{arr} is the arrival time of each photon, t_{TTS} is the TTS of MCP-PMT, and $v(t)$ is the single photoelectron (SPE) response function, which is obtained by fitting the waveform of MCP-PMT as shown in Fig. 11 [13]. Note that the time jitter of electronics is neglected.

4.2. Simulation results

We first simulate the transmission process of Cherenkov photons in the MCP-PMT without any external radiator (marked as "TCw" in Figs. 12 and 13) where the Cherenkov photons are generated in PMT's window. The arrival time of Cherenkov photons versus its hit position (the hit radius from the center of MCP-PMT's photocathode) is shown in Fig. 12(a). The lowest arrival time band is from the direct-hit photons, which reach the photocathode directly without any reflection, and photons of all other bands in Fig. 12(a) have experienced one or more reflections. It is easy to evaluate the "Full Signal" region: R < 2.5 mm, where the reflected band starts, with a time resolution about 3.8 ps ± 0.019 (as shown in Fig. 13). In the region of 2.5 mm < R < 9 mm where the lowest band ends, there are the "Partial Signals". Due to the increased reflections, the time resolution gets worse and forms a peak at R > 7 mm (Fig. 13). At R > 9 mm only diffused reflected photons reach the photocathode, there are the "Reflected Signals".

In the cases of TC0 and TC1 with external radiator, the Cherenkov photons are generated in both the external radiator and the window of PMT. Obviously, the external radiator raises the number of photo-electrons (NPE) induced in the photocathode at R < 2.5 mm (TC0) and R < 6 mm (TC1) as shown in the upper plot of Fig. 13. According to Fig. 12(b, c), the increased NPE comes from both Cherenkov direct-hit photons and reflected photons. The former improves the time resolution while the latter worsens it. Therefore TC0 has a better time resolution than TCw at R < 2.5 mm where the direct-hit photons dominate, while TC1 has a slight improvement at R < 6 mm as it has more reflected photons. Note that there is an obvious peak at 2.5 mm < R < 3.5 mm for the TC0. It is because the Cherenkov cone generated in the radiator is close to the radiator boundary (at R of 3 mm), the number of reflected photons strongly increased and cause large time fluctuation.

In conclusion, an incident particle passing through the radiator closer to PMT's photocathode can generate more direct-hit photons, and get better time resolution. This explains the position dependence of the prototype's time resolution. A reasonable way to verify this dependence is to use NPE as the threshold to select signals dominated by direct-hit photons. Fig. 14 shows the time resolution dependent on the NPE threshold. Black circles and red squares are beam test results sampled by oscilloscope and simulation result respectively. NPE is evaluated by comparing the signal's charge with SPE's. Obviously, the higher NPE threshold effectively improves the time resolution, the best time resolution is achieved at the NPE threshold of 50: $\sigma_{\text{T1-T0,MC}}$ = 4.6 ps; $\sigma_{\text{T1-T0,Exp}}$ = 5.1 ps. It agrees with the simulation result in Fig. 13, both plots show a good time resolution with NPE above 50.

5. Summary

A prototype of picosecond timing counter consisted of a Cherenkov radiator attached to MCP-PMT and readout by FPGA-based multi-threshold leading-edge timing electronics has been developed. The beam test shows that it can achieve a time resolution of 9.8 ps. To analyze the test results, a GEANT4 simulation is performed to study the prototype's working mechanism, especially the position dependence of its time resolution. The simulation result agrees with the beam test and shows that Cherenkov photons which directly hit within the PMT's photocathode region have the best timing performance. Therefore, adding an appropriate focus lens between the external radiator and the MCP-PMT may be an easy and reasonable way to improve the timing performance of the prototype.

Declaration of competing interest

The authors declare that they have no known competing financial interests or personal relationships that could have appeared to influence the work reported in this paper.

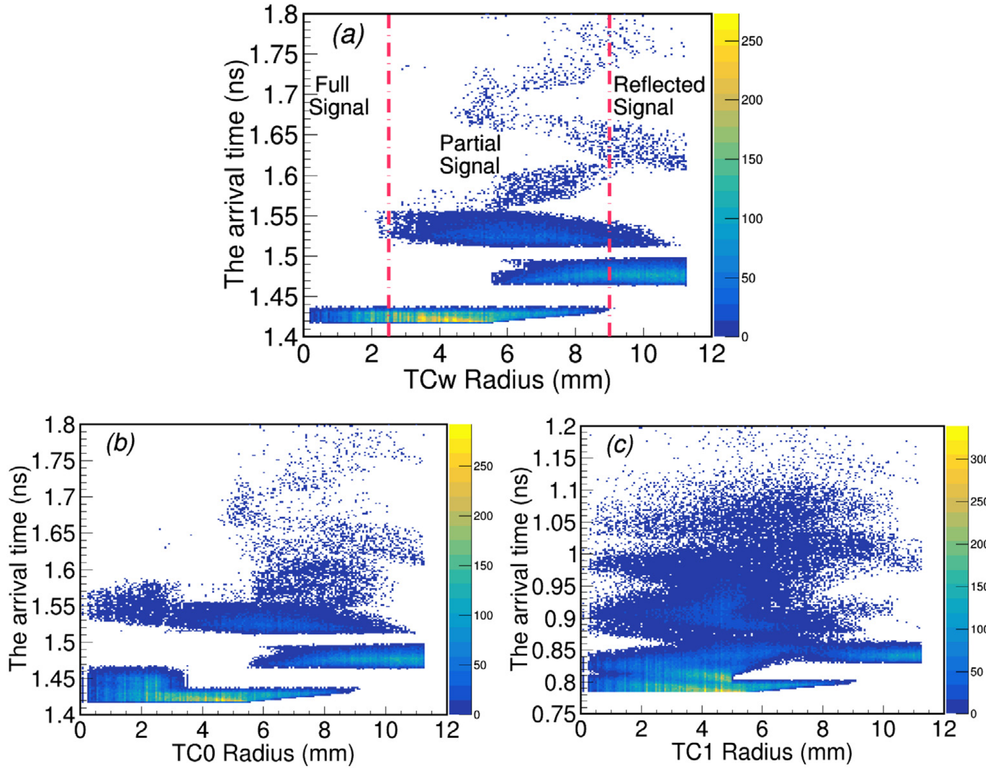

Fig. 12. The distribution of the arrival time along the radius from the center of MCP-PMT's active area: TCw(a), TC0 (b) and TC1(c).

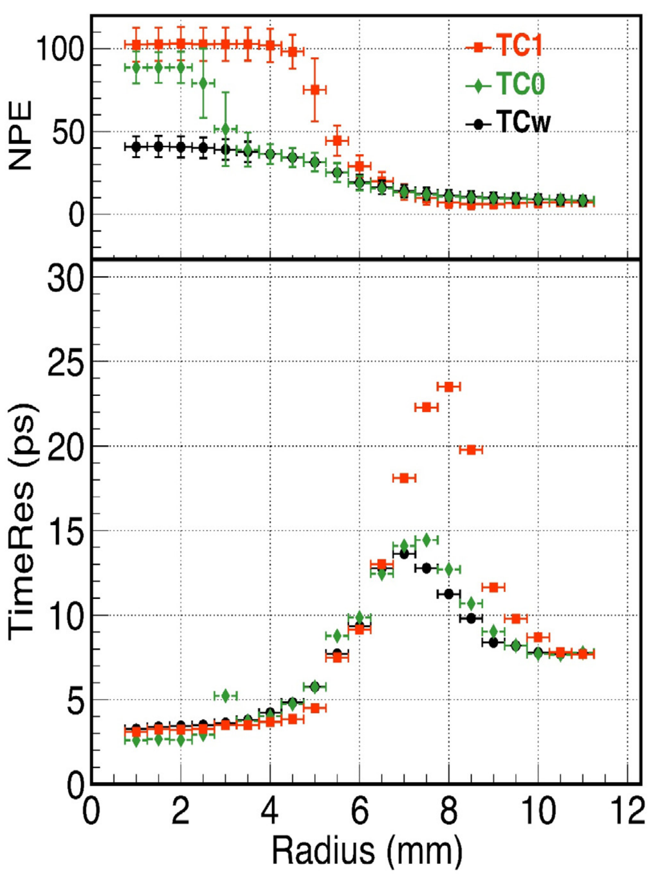

Fig. 13. The time resolution as a function of radius and the smaller plot a zoom for the inner radii: TCw (black dot), TC0 (green diamond) and TC1 (red square). The corresponded number of photoelectrons in the upper panel.

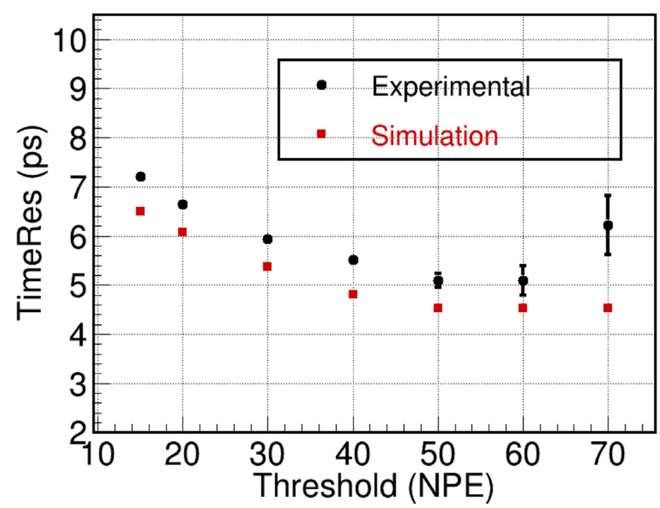

Fig. 14. Timing resolution dependence on the NPE threshold. Black circle and red square are experimental and simulation results respectively. MCP is working at 3300 V and using 30% CFD as a threshold.

CRediT authorship contribution statement

Ziwei Li: Writing - original draft, Software, Formal analysis, Validation, Investigation. **Xin Li:** Conceptualization, Methodology, Investigation, Validation, Writing - review & editing, Funding acquisition. **Qiang Cao:** Software, Validation, Data curation, Writing - review & editing. **Cheng Li:** Conceptualization, Methodology, Writing - review & editing, Funding acquisition. **Yonggang Wang:** Conceptualization, Methodology, Resources. **Jianbei Liu:** Conceptualization, Methodology, Project administration. **Ming Shao:** Conceptualization, Methodology, Writing -

review & editing. **Haiping Peng:** Conceptualization, Methodology, Visualization. **Xu Wang:** Investigation, Resources. **Yi Zhou:** Investigation, Resources. **Zhengguo Zhao:** Supervision, Project administration.

Acknowledgments

This research work is supported by the National Natural Science Foundation of China, No. 11775217, 11675172. Special thanks for all help and supports from CERN/RD51 group and USTC colleagues.

References

[1] Martin Aleksa, et al., Strategic R & D, Programme on Technologies for Future Experiments. No. CERN-OPEN-2018-006, 2018.
[2] L. Linssen, Technological challenges of future HEP experiments, Presentation, Open Symposium, Granada, Spain (13-16 2019).
[3] CLICdp Collaboration, Detector Technologies for CLIC, CERN Yellow Reports: Monographs, 2019, http://cds.cern.ch/record/2673779.
[4] CMS collaboration, Technical Proposal for the Phase-II Upgrade of the CMS Detector, CMS Technical proposal CERN-LHCC-2015-010, CMS-TDR-15-02, CERN, 2015.
[5] Neville Harnew, et al., Status of the TORCH time-of-flight project, Nucl. Instrum. Methods Phys. Res. A 952 (2020) 161692.
[6] Hamamatsu Photonics, Microchannel Plate- Photomultiplier TubeS (MCP-PMT), R3809U-50 Series, 2015, https://www.hamamatsu.com/resources/pdf/etd/R3809U-50_TPMH1067E.pdf.
[7] Nicola Minafra, et al., Test of ultra-fast silicon detectors for picosecond time measurements with a new multipurpose read-out board, Nucl. Instrum. Methods Phys. Res. A 867 (2017) 88–92.
[8] Yonggang Wang, et al., A 3.9-ps RMS precision time-to-digital converter using ones-counter encoding scheme in a kintex-7 FPGA, IEEE Trans. Nucl. Sci. 64 (10) (2017) 2713–2718.
[9] Qiang Cao, et al., FPGA based picosecond time measurement system for a DIRC-like TOF detector, 2018, arXiv preprint arXiv:1806.02495.
[10] L. Sohl, Spatial time resolution of MCP–PMTs as a t0-reference, Nucl. Instrum. Methods Phys. Res. A (2018).
[11] Geant4 Collaboration, Geant4 User'S Guide for Application Developers, Version geant4 9, 2009.
[12] Li. Xin, et al., Effect of light transmission characteristic of scintillator on the intrinsic time resolution of ETOF, High Energy Phys. Nucl. Phys. 30 (10) (2006) 1001–1005.
[13] T. Ishikawa, et al., Charge-to-time converting leading-edge discriminator for plastic-scintillator signals, Nucl. Instrum. Methods Phys. Res. A 875 (2017) 193–200.